Active Control and Parameter Updating Techniques for Nonlinear Thermal Network Models

Miltiadis V. Papalexandris, Mark H. Milman

Jet Propulsion Laboratory,
California Institute of Technology,
Pasadena, CA 91109

Abstract

The present article reports on active control and parameter updating techniques for thermal models based on the network approach. Emphasis is placed on applications where radiation plays a dominant role. Examples of such applications are the thermal design and modeling of spacecrafts and space-based science instruments. Active thermal control of a system aims to approximate a desired temperature distribution or to minimize a suitably defined temperature-dependent functional. Similarly, parameter updating aims to update the values of certain parameters of the thermal model so that the output approximates a distribution obtained through direct measurements. Both problems are formulated as nonlinear least-squares optimization problems and a general framework is developed for their study. Certain theoretical questions associated with these problems, such as existence of solutions, are examined. The proposed optimization strategies are explained in detail and their efficiency is demonstrated through a series of numerical tests.

1. Introduction

Thermal modeling and analysis is a critical component of many engineering systems. The various numerical techniques that have been developed over the years for this purpose can be divided in two main categories; finite-element and finite-difference techniques. They are both derived from discretizations of the underlying heat-transfer equation. Among them, one of the most popular techniques is the thermal network (or lumped-parameter) approach. This approach is derived from a particular finite-difference discretization of the governing equation. According to this method, the system is partitioned to isothermal nodes with pointwise properties that can exchange heat either by conduction or radiation. The main advantages of the thermal network approach are flexibility and straightforward implementation of components with complicated geometry.

The present work is concerned with two particular aspects of thermal modeling, active control and parameter updating on network models. The importance of these two aspects has increased in the recent years due to high precision and/or stability requirements of modern applications. The objective of active control is to achieve a desired temperature profile via addition or subtraction of heat. On the other hand, the objective of model updating is to update the values of various parameters of the thermal model so that the numerically computed temperature profiles match actual test data; *i.e.*, it aims to improve the fidelity of the model.

The first part of this paer deals with certain theoretical results, such as existence of solutions to the problems of interest with and without constraints, and smoothness of the solution paths. Thermal network properties are exploited to derive these results. In the second part of the article, the proposed algorithms are described in detail, and their efficiency is demonstrated through tests on large-scale spacecraft models that have been used in ongoing NASA projects.

It is worth mentioning that during the course of this study a computational framework has been developed for the numerical treatment of the problems of interest. Particular effort was devoted to make this framework suitable for integrated modeling. This is a methodology where multidisciplinary models are developed for the design and analysis of engineering systems. Typical examples of systems with high demand for integrated modeling include spacecrafts and other aerospace applications.

Integrated modeling is emerging as an indispensable tool in modern engineering practice because it simplifies significantly the analysis of very complicated systems. Furthermore, it allows the study of various internal and external factors, and their impact on the system of interest, even during the early design stages. In many projects, accurate thermal analysis is considered a critical component of this methodology. Although modeling tools from areas such as structural mechanics and automated control have been successfully integrated into this process, the thermal analysis discipline has been integrated in less extent.

2. Description of the thermal network model

A thermal network is defined by a set of nodes that are connected to each other via linear or quartic conductances, and is analogous to electrical networks, Dusinberre [1], Birkhoff & Kellogg [2]. In principle, a thermal network model arises from a finite-difference discretization of the steady-state, heat-transfer equation,

$$\nabla \cdot (k \nabla T) \;=\; f\,, \tag{1}$$

where k is the thermal conductivity, T is the temperature, and f is the heat load. In many occasions, however, the network approach is adopted to construct models of complex systems in which a node is merely an isothermal component and is not derived from discretization of equation (1).

In general, a thermal network model consists of N internal nodes and n boundary nodes. The temperature distribution on the boundary is assumed to be known and given. The finite-difference discretization of (1) reduces to the following set of N nonlinear algebraic equations,

$$\hat{Q}_i + \sum_{j=1}^{N+n} \hat{C}_{ij}(T_j - T_i) \;+\; \sum_{j=1}^{N+n} \hat{R}_{ij}(T_j^4 - T_i^4) \;=\; 0\,,\;\; i = 1, \ldots, N\,. \tag{2}$$

In the above equations, $\hat{Q}_i$ are the heat loads of the system, while $\hat{C}_{ij}$ and $\hat{R}_{ij}$ are the conduction and radiation coefficients of the system, respectively.

The conduction coefficients are given by Fourier's law,

$$\hat{C}_{ij} = \frac{kA}{L}, \tag{3}$$

where k is the thermal conductivity of the material (it can be either constant or temperature dependent), A is the cross-sectional area of heat flow, and L is the length between nodes i and j. Convection conductors are computed from the expression

$$\hat{C}_{ij} = hA, \tag{4}$$

where h is the convective heat transfer coefficient and A is the surface area in contact with the fluid. On the other hand, the radiation coefficients are given by

$$\hat{R}_{ij} = \sigma A \varepsilon, \tag{5}$$

where σ is the Stephan-Boltzmann constant, A is the area that corresponds to node i, and ε is the emissivity between nodes i and j.

The system (2) can be written as a matrix equation after the following substitutions. First, let $T = [T_1, \ldots, T_N]^{\mathrm{T}}$ and $D(T) = [T_1^4, \ldots, T_N^4]^{\mathrm{T}}$. Further, define the $N \times N$ matrices C and R as

$$C_{ij} = \begin{cases} \hat{C}_{ij}, & \text{if } i \neq j, \\ -\sum_{j=1}^{N+n} \hat{C}_{ij}, & \text{if } i = j, \end{cases} \tag{6}$$

and

$$R_{ij} = \begin{cases} \hat{R}_{ij}, & \text{if } i \neq j, \\ -\sum_{j=1}^{N+n} \hat{R}_{ij}, & \text{if } i = j. \end{cases} \tag{7}$$

Finally, let $Q = [Q_1, \ldots, Q_N]^{\mathrm{T}}$ be the forcing vector of the system (2), arising from the combination of the heat loads $\hat{Q}_i$, and the energy exchange through the boundary nodes. In other words,

$$Q_i = \hat{Q}_i + \tilde{Q}_i, \quad i = 1, \ldots, N, \tag{8}$$

with

$$\tilde{Q}_i = \sum_{j=N+1}^{N+n} \hat{C}_{ij} T_j + \sum_{j=N+1}^{N+n} \hat{R}_{ij} T_j^4, \quad i = 1, \ldots, N. \tag{9}$$

After making these substitutions, the thermal network equation (2) is written in the more compact form

$$F(T) \equiv Q + CT + RD(T) = 0\,. \tag{10}$$

Methods, and their theoretical foundations, for solving general systems of nonlinear equations are described by Rheinboldt, [3] Algorithms developed specifically for the thermal network model (10) have been proposed, among others, by Milman & Petrick [4], Krishnaprakas [5], *e.t.c.*

3. Formulation of the control and parameter updating problems

This section is devoted to the description and formulation of the active control and parameter updating problems. The following definitions are necessary for the discussion that follows. Let $\mathbb{R}^N$ be the real, N-dimensional linear space of column vectors $x = (x_1, \dots, x_N)^{\mathrm{T}}$. The coordinate-wise partial ordering on $\mathbb{R}^N$ implies that if $x, y \in \mathbb{R}^N$, then $x \geq y$ if and only if $x_i \geq y_i$ for all $i = 1, \dots, N$. The l_∞-norm, $|x| = \max\{|x_i| : i = 1, \dots, N\}$, in $\mathbb{R}^N$ will also be used. Further, let $\mathbb{R}^N_+ = \{x \in \mathbb{R}^N : x \geq 0\}$. Finally, in the sequel, it will be assumed that both linear and radiation conductances of the system are constant.

Suppose that there are $m \leq N$ nodes in the system (10) whose temperatures have to be controlled. For simplicity assume that these are the first m nodes of the system and denote by $T_\alpha \in \mathbb{R}^m_+$ their temperature vector. Also, consider a target temperature profile $T_0 \in \mathbb{R}^m_+$ and a least-square type objective function w associated with T_α,

$$w(T_\alpha) = \Big[(T_\alpha - T_0)^{\mathrm{T}} \cdot E \cdot (T_\alpha - T_0)\Big]^{1/2}\,. \tag{11}$$

In the above equation E is an $m \times m$ constant, positive definite matrix. The purpose of thermal control is to achieve a distribution T_α such that w attains a minimum. The control action is provided by the thermal-load vector $\hat{Q} \in \mathbb{R}^m$, assigned to the m nodes of interest. Therefore, the active control problem is formulated as a nonlinear, least-squares minimization problem with constraints with respect to the objective function w as follows.

$$\min_{\hat{Q}} w(\hat{Q}) = \left[\Big(\hat{Q}(T_\alpha) - T_0\Big)^{\mathrm{T}} \cdot E \cdot \Big(\hat{Q}(T_\alpha) - T_0\Big)\right]^{1/2}, \tag{12}$$

subject to $2(m+1)$ constraints:

$$\begin{aligned} b_i^{\mathrm{L}} \leq\ & Q_i \leq b_i^{\mathrm{U}}\,, \quad i = 1, \dots, m\,, \\ Q_{\mathrm{MIN}} \leq\ & \sum_{i=1}^{m} Q_i \leq Q_{\mathrm{MAX}}\,, \end{aligned} \tag{13}$$

where $\sum b_i^{\mathrm{L}} \leq Q_{\mathrm{MIN}}$ and $Q_{\mathrm{MAX}} \leq \sum b_i^{\mathrm{U}}$. These constraints express practical limitations in the available power that can be produced by the heaters or coolers of the system.

In the parameter updating problem the goal is to modify the values of certain physical parameters of the network model so that the numerically computed temperature distribution at $m \leq N$ nodes of interest, denoted by T_α, is as close as possible to a target profile T_0. In other words, the solution for the first m equations of the system (10) must be as close as possible to T_0. The parameters that have to be estimated are usually the conductivities k of the linear conduction coefficients, equation (3), and the emissivities ε of the radiation coefficients, equation (5). The emissivities, in particular, are very sensitive to various factors, such as roughness of the radiative surfaces, ambient temperature and others, whose effect is difficult to be measured with precision. The target profile T_0 consists of experimental or measured test data.

Assume that there are M parameters of interest, conductivities and emissivities. Given the dimensions of the matrices C and R, the maximum possible value of M is $2N^2$. These matrices, however, are usually sparse. Furthermore, the parameters of interest are material properties, which means that each parameter is associated to a whole cluster of coefficients. Therefore, in practice, M is much smaller than $2N^2$.

Denote by $\Omega \in \mathbb{R}^M$ the set of parameters (conductivities and/or emissivities) that have to be estimated. Then, the parameter updating problem is formulated as a constrained, least-square optimization problem,

$$\min_{\Omega} w(\Omega) = \left[\sum_{i=1}^{m} \left(T_{\alpha_i}(\Omega) - T_{0_i} \right)^2 \right]^{1/2}, \tag{14}$$

subject to the following $2M$ constraints,

$$B_i^{\mathrm{L}} \leq \Omega_i \leq B_i^{\mathrm{U}}, \quad i = 1, \ldots, M. \tag{15}$$

These constraints express certain physical limitations on the values of the parameters of interest. One such obvious constraint is that these parameters have to be strictly positive, that is $\Omega > 0$. Other restrictions might hold, too. For example, the emissivities ε must be strictly positive but smaller than 1. The above formulation of parameter updating as an optimization problem was previously considered by Narayana *et al.*, [6], who employed the simplex method for its solution.

3. Solvability of the control and parameter updating problems

In this section, some results pertaining to the solvability of the optimization problems described above are presented. Besides their theoretical interest, these results provide useful insight about the accuracy and robustness of the numerical procedures that may be employed for the solution of the problems under consideration.

Certain important properties of thermal networks play the key role for the derivation of these results. For example, the conduction matrices, C and R of such networks, hence their sum, are by construction diagonally dominant with negative values in the diagonal. A matrix $U = (u_{ij})$ is diagonally dominant if $\sum_{i \neq j} |u_{ij}| \leq |u_{ii}|$. When strict inequality holds for all i, then the matrix is said to be strictly diagonally dominant.

Furthermore, in thermal networks each node can exchange energy with any other node through a sequence of nodes connected by a combination of conductors and/or radiators. This implies that the directed graph of the matrix $C+R$ is strongly connected, *i.e.*, $C+R$ is irreducible, Varga [7]. Also, in network models at least one internal node is connected to a boundary node with nonzero interchange factor. This means that $C+R$ has a strict diagonal dominance in the corresponding row. In this case, $C+R$ is said to be *irreducibly dominant.*

Finally, another important property of the system (10) that arises directly from the structure of $C+R$ is the coercivity of $F(T)$ for fixed Q; see [4], Lemma 2.1. The coercivity property implies that if $\{T_n\}$ is a sequence with non-negative components and $|T_n| \to \infty$, then $|F(T_n)| \to \infty$. It is a manifestation of the fact that the energy balance can not be satisfied for arbitrary large temperatures.

The theorem that establishes existence and uniqueness of solution to the general system (10) can be found in [4]. It is presented below, without proof, for completion purposes.

Theorem 1. *Suppose that C and R are symmetric, non-positive matrices with $C+R$ irreducibly dominant. Then, if Q is nonzero with $Q \geq 0$, the system (10) has a unique solution T^* with* $T^* > 0$. (Milman & Petrick, [4]).

The requirement that $C+R$ be irreducibly dominant is essential for the existence of solutions of the system (10). In particular, the invertibility of the Jacobian of the system,

$$\frac{\partial F}{\partial T} = (C + RD'(T)) \, , \tag{16}$$

where $D'(T) = [4T_1^3, \ldots, 4T_N^3]^{\mathrm{T}}$, is a direct consequence of this requirement.

The following two lemmas are necessary for the derivation of the main results of this section. The first lemma is a generalization of the theorem above for a particular class of networks that consist of subsystems that are not necessarily connected to each other.

Lemma 1. *Suppose that C and R are symmetric, non-positive matrices with $C+R$ diagonally dominant and reducible. If all the diagonal submatrices of the normal form of $C+R$ are connected to a boundary node, then the system (10) has a unique solution $T^* > 0$, for every $Q \geq 0$.*

Proof. It is known, Varga [7], that for every reducible $n \times n$ matrix A, there is an $n \times n$ permutation matrix P such that

$$PAP^{\mathrm{T}} = \begin{bmatrix} B_{11} & B_{12} & \cdots & B_{1m} \\ 0 & B_{22} & \cdots & B_{2m} \\ \vdots & \vdots & & \vdots \\ 0 & 0 & \cdots & B_{mm} \end{bmatrix} , \tag{17}$$

where each square submatrix B_{jj}, $1 \leq j \leq r < N$, is irreducible. The matrix PAP^{T} is called the normal form of A. Note that C and R are both assumed to be symmetric, therefore, their sum is also symmetric. This implies that the normal form of $C + R$ is a block-diagonal matrix,

$$P(C+R)P^{\mathrm{T}} = \begin{bmatrix} B_{11} & 0 & \cdots & 0 \\ 0 & B_{22} & \cdots & 0 \\ \vdots & \vdots & & \vdots \\ 0 & 0 & \cdots & B_{mm} \end{bmatrix}, \tag{18}$$

with every diagonal block B_{jj}, $1 \leq j \leq r$, being irreducible and diagonally dominant. If for every B_{jj} there is at least one node that is connected to a boundary node or has a heat load applied to it, then all the matrices B_{jj}, $1 \leq j \leq r$, are irreducibly dominant. Consequently, Theorem 1 can be applied to each of the subsystems of the large system (10).///

This lemma implies that Theorem 1 holds for thermal networks which can be partitioned to subsystems that are not connected to each other, provided that each of these subsystems experiences some kind of energy exchange with its environment. In other words, this condition requires that none of the subsystems is thermally isolated.

The second lemma that is required is the following.

Lemma 2. Any principal submatrix $\hat{U}$ of a symmetric, irreducibly dominant matrix U, is either irreducibly dominant or its normal form is block-diagonal with irreducibly dominant blocks.

Proof. $\hat{U}$ is obviously symmetric, and diagonally dominant. If it is irreducible, then the lemma holds. If it is not, then it can be shown, by following the same argument as in Lemma 1, that the normal form of $\hat{U}$ is block-diagonal and all the diagonal blocks are symmetric, diagonally dominant and irreducible. It remains to show that each diagonal block is irreducibly dominant.

Moré, [8], has shown that any principal submatrix of an irreducibly dominant matrix is invertible. Therefore, all the diagonal blocks of the normal form $\hat{U}$ are invertible, which implies that their determinant is non-zero. Assume that a diagonal block of $\hat{U}$, say $\hat{u}$, is not irreducibly dominant. Since $\hat{u}$ is diagonally dominant, then $\hat{u} \times [1, \ldots, 1]^{\mathrm{T}} = 0$. This means that the determinant of $\hat{u}$ is zero, which is impossible because it contradicts the invertibility of $\hat{u}$.///

Subsequently, let the system (10) be written in the form

$$\begin{bmatrix} \hat{Q} \\ 0 \end{bmatrix} = -\begin{bmatrix} \tilde{Q}_\alpha \\ \tilde{Q}_\beta \end{bmatrix} - \begin{bmatrix} C_{\alpha\alpha} & C_{\alpha\beta} \\ C_{\beta\alpha} & C_{\beta\beta} \end{bmatrix} \begin{bmatrix} T_\alpha \\ T_\beta \end{bmatrix} - \begin{bmatrix} R_{\alpha\alpha} & R_{\alpha\beta} \\ R_{\beta\alpha} & R_{\beta\beta} \end{bmatrix} \begin{bmatrix} D(T_\alpha) \\ D(T_\beta) \end{bmatrix}. \tag{19}$$

where $T = [T_\alpha \; T_\beta]^{\mathrm{T}}$, and $C_{\alpha\alpha}$, $R_{\alpha\alpha}$ are $m \times m$ principal submatrices of C and R, respectively. $C_{\beta\beta}$ and $R_{\beta\beta}$ are also principal submatrices of C and R, of dimension $(n-m) \times (n-m)$.

Finally, since C and R are symmetric, then $C_{\beta\alpha} = C^{\mathrm{T}}_{\alpha\beta}$ and $R_{\beta\alpha} = R^{\mathrm{T}}_{\alpha\beta}$. In the sequel, the following abbreviated form of equation (19) will also be used,

$$\hat{Q} = F_{\alpha\alpha}(T_\alpha) + F_{\alpha\beta}(T_\beta) , \tag{20}$$
$$0 = F_{\beta\alpha}(T_\alpha) + F_{\beta\beta}(T_\beta) , \tag{21}$$

where

$$F_{ii}(T_i) = -C_{ii}T_i - R_{ii}D(T_i) , \qquad i = \alpha, \beta, \tag{22}$$
$$F_{ij}(T_j) = -C_{ij}T_j - R_{ij}D(T_j) - Q_i , \qquad i, j = \alpha, \beta, \;\; i \neq j. \tag{23}$$

The following theorem is one of the two main results of this section. It establishes controllability of the system (19). Controllability implies that the system (20) can attain any desired temperature distribution T, provided that the appropriate heat load $\hat{Q}$ is applied to it. For steady-stare problems like the one examined in the present work, the controllability property is equivalent to solvability of the *unconstrained* minimization problem (12).

Theorem 2. *Suppose that C and R are symmetric, non-positive, matrices and $C + R$ is irreducibly dominant. Then, for every $T_\alpha \in I\!R^m$ with $T_\alpha > 0$, the subsystem (20) has a unique solution $\hat{Q} \in I\!R^m$ which is independent of T_β.*

Proof. Consider the subsystem (21) and observe that both $C_{\beta\alpha}$ and $R_{\beta\alpha}$ consist of off-diagonal elements of C and R, respectively. Therefore, all their elements are non-negative. Since $T_\alpha > 0$, it follows that $F_{\beta\alpha}(T_\alpha) \leq 0$. On the other hand, $C + R$ is irreducibly dominant, hence Lemma 2 can be applied to its principal submatrix $C_{\alpha\alpha} + R_{\alpha\alpha}$. Therefore, according to Lemma 1, the subsystem (21) has a unique solution, say $T_\beta > 0$. This solution is given as a function of T_α by

$$T_\beta = F^{-1}_{\beta\beta}(-F_{\beta\alpha}(T_\alpha)) . \tag{24}$$

The solution (24) can be substituted into the subsystem (20), yielding the following expression for $\hat{Q}$:

$$\hat{Q} = F_{\alpha\alpha}(T_\alpha) + F_{\alpha\beta}\left(F^{-1}_{\beta\beta}(-F_{\beta\alpha}(T_\alpha))\right) . \tag{25}$$

This solution exists for every $T_\alpha > 0$. The uniqueness of $\hat{Q}$ follows immediately from (20).///

As far as the inverse mapping is concerned, it is useful to mention that the following theorem reduces the dimensionality of the system under consideration.

Theorem 3. *Suppose that C and R are symmetric, non-positive matrices and $C + R$ is irreducibly dominant. Then, for every $\hat{Q} \in I\!R^m_+$ with $\hat{Q} \geq 0$, the system (20)-(21) can be reduced to an m-dimensional mapping $\tilde{F}^{-1} : \hat{Q} \to T_\alpha$, which is diffeomorphic on $I\!R^m_+$.*

Proof. The theorem is based on the construction of solution paths for the subsystem (21) through Lemmas 1 and 2. Solution paths for the subsystem (20) are generated by a simple homotopy idea, similar to the one employed in [4] for the proof of Theorem 1.

Consider an arbitrary $\hat{Q}^{\circ} \geq 0$. According to Theorem 1, the system (20)-(21) has a unique solution, say $T^{\circ} = [T_{\alpha}^{\circ}\ T_{\beta}^{\circ}]^{\mathrm{T}}$. The fact that $C + R$ is irreducibly dominant, in combination with Lemmas 1 and 2, asserts that for every $T_{\alpha} > 0$ there exists a unique solution $T_{\beta} > 0$ that solves the subsystem (21). This solution can be written as

$$T_{\beta} = F_{\beta\beta}^{-1}(-F_{\beta\alpha}(T_{\alpha})) \equiv \tilde{F}_{\beta}(T_{\alpha}) . \tag{26}$$

Since $F_{\beta\alpha}, F_{\beta\beta}$ are C^{∞} mappings, $\tilde{F}_{\beta}$ is also a C^{∞} mapping, according to the inverse function theorem. Substitution of (26) into (20), produces the following relation

$$\hat{Q} = F_{\alpha\alpha}(T_{\alpha}) + F_{\alpha\beta}\left(F_{\beta\beta}^{-1}(-F_{\beta\alpha}(T_{\alpha}))\right) \equiv \tilde{F}(T_{\alpha}) , \tag{27}$$

which holds as long as $T_{\alpha} > 0$. Obviously it holds in a neighborhood of T_{α}°. Since the Jacobian of the system (20)-(21) and the Jacobian of the subsystem (21) are both invertible at $(T_{\alpha}^{\circ}, T_{\beta}^{\circ})$, then from Keller [9], Lemma 4.9, it follows that the Jacobian of $\tilde{F}$ is also invertible at T_{α}°. Furthermore, all the F_{ij} functions that appear in (27) are C^{∞} mappings, hence $\tilde{F}$ also belongs to this class. Therefore, by virtue of the inverse function theorem, $\tilde{F}$ defines a diffeomorphism onto an open neighborhood of T_{α}°.

Let $\tilde{F}^{-1}$ be the inverse of $\tilde{F}$ in the neighborhood of T_{α}°, and for $\lambda \in [0, 1]$ define the function

$$H(T_{\alpha}^{\circ}, \lambda) = Q^{\circ} + \lambda(Q - Q^{\circ}) - F_{\alpha\alpha}(T_{\alpha}) - F_{\alpha\beta}\left(F_{\beta\beta}^{-1}(-F_{\beta\alpha}(T_{\alpha}))\right) . \tag{28}$$

It is true that $H(T_{\alpha}^{\circ}, 0) = 0$ and the original problem is to solve $H(T_{\alpha}, 1) = 0$. This implies that the solution paths of

$$H(T_{\alpha}, \lambda) = 0 , \tag{29}$$

can be continued from $\lambda = 0$ to $\lambda = 1$. But the implicit function theorem asserts that equation (28) can be solved locally in a neighborhood of $\lambda > 0$ to produce a smooth solution curve. This curve can be continued as long as $\partial H / \partial T_{\alpha}$ stays nonsingular. According to the above, this happens as long as $T_{\alpha} > 0$. On the other hand, Theorem 1 requires that solutions of (20)-(21) be positive for any $\hat{Q} > 0$, hence T_{α} remains always positive.

Therefore, the solution path of (26) is a one-dimensional manifold. The solution curve $T_{\alpha}(\lambda)$ is diffeomorphic to the real line since the Jacobian of $\tilde{F}$ stays invertible, and thereby unique solutions of (26) exist in every (T_{α}, λ) neighborhood of the solution. The path $T_{\alpha}(\lambda)$ can not be continued to $\lambda = 1$ only if the solution blows up for some $\lambda^{*} \in [0, 1]$. But this is impossible because of the coercivity of the combined system (20)-(21), [4]. Uniqueness of the solutions T_{α} of (20) follows immediately from the uniqueness of the solution of the combined system.///

Note that the mapping $\hat{Q} = \tilde{F}(T_{\alpha})$ is a smooth function defined on a compact subset of $\mathbb{R}^{m}$. Therefore, existence of solutions to the constrained optimization problem (12)-(13) follows immediately. Existence of solutions to the parameter updating problem (14)-(15) can be established in the same, straightforward manner. First, observe that the constraints (15) define a compact subset of $I\!R^M$. Then, consider any initial estimate of the parameter vector $\Omega^o > 0$ from this subset. According to theorem 1, the system $F(T;\Omega) = 0$, equation (10), has a unique solution $T^o = [T^o_\alpha, T^o_\beta] > 0$. The Jacobian of the system, $\partial F/\partial T$, is non-zero and finite at T^o. By the implicit function theorem, the system (10) can be solved locally to produce a smooth solution curve $[T_\alpha, T_\beta] = S(\Omega) = [S_\alpha(\Omega), S_\beta(\Omega)]$ in a neighborhood of T^o. This curve can be continued so long as the $\partial F/\partial T$ remains invertible. This happens for all $T > 0$. In other words, $S_\alpha(\Omega)$ defines a smooth mapping from a compact subset of $I\!R^M$ to a compact subset of $I\!R^m$, hence there exists a solution to the problem (14)-(15).

5. Implementation of the algorithm

As mentioned in section 3, both the thermal control problem, equations (12)-(13), and the parameter updating problem, equations (14)-(15), are formulated as nonlinear optimization problems with constraints. Their solutions satisfy the well-known optimality conditions of Kuhn-Tucker; see, for example, Bryson & Ho [10], or Gill *et al.* [11],

$$\frac{\partial w}{\partial T_i} - \sum_{j=1}^{M} u_j \frac{\partial f_j}{\partial T_i} = 0 , \quad i = 1, \dots , m , \tag{30}$$

$$u_j \cdot f_j(T) = 0 , \quad j = 1, \dots , M , \tag{31}$$

$$f_j(T) \leq 0 , \quad j = 1, \dots , M . \tag{32}$$

In the above relations, f_j and u_j, $j = 1, \dots , M$, are the constraints, expressed in a general form by equation (32), and the Lagrange multipliers of the problem, respectively.

Over the years, numerous algorithms have been developed for the numerical solutions of such optimization problems. The literature on the topic is vast; see, for example, [11], and references therein. Most of these algorithms are based on some suitable iterative procedure to identify points where conditions (30)-(32) are satisfied.

Among them, the Sequential Quadratic Programming method (SQP), Han [12], Powell [13], is considered one of the most effective and reliable methods for nonlinear optimization. It has been employed for the particular problems under consideration of the present study. The algorithms that solve the optimization programs of interest have been implemented in a MATLAB code. The code is based on the built-in SQP routine of MATLAB, [14].

The SQP method requires the computation of the solution of the system (10) and its Jacobian during each step of the iteration procedure. In the present study, this system is solved with the algorithm described in [4]. It is based on a restricted stepsize Newton method, [4]. The Newton iterates are evaluated along descent direction for $|F(T)|^2$. The stepsize of each iteration is determined via the line-search algorithm, [16]. A very powerful feature of the thermal solver is the analytic evaluation of the Jacobian of the system (16).

The elimination of finite-differencing procedures for the evaluation of derivatives accelerates the convergence rate of the algorithm and offers considerable computing-time savings. The algorithm is implemented in MATLAB and is part of IMOS (Integrated Modeling of Optical Systems), a computational environment that was developed at JPL, [15].

Another issue of the active control problem that merits discussion is that quite often the number of the available heaters, say q, is less than the number of nodes, m, that affect the objective function (11). In such cases, the location of the $q < m$ heaters must be selected. This can be performed by ranking of the contribution of the m heaters to the performance index. This ranking can be implemented via the following procedure. First, the eigenvalues, e_i, and left eigenvectors v_i, $i = 1, \ldots, m$ of the $m \times m$ matrix E appearing in (11) are determined. Then, the vector V, defined as

$$V = \sum_{i=1}^{m} e_i \cdot v_i \, . \tag{33}$$

is computed. The elements of V are subsequently ranked according to their absolute values. This ranking gives a measure of the relative importance of the m nodes to the index w. The top q nodes of the ranking determine the locations where heaters will be applied.

6. Numerical Examples

The thermal control algorithm has been applied to a network model of the Next Generation Space Telescope (NGST), shown in Figure 1. The model consists of $N = 1802$ internal nodes and $n = 48$ boundary nodes. There are more than 5800 linear conductors and more than 160,000 radiation conductors. It was prepared by the NASA Goddard and NASA Marshall space centers.

Thermal analysis is a particularly essential issue in the design of space telescopes, because of their sensitivity to temperature variations. The most important heat load applied on the telescope is radiation from the sun and the earth. The amount of radiated heat varies considerably as the telescope rotates to aim at different parts of the sky. Significant temperature variations (a few degrees Kelvin) on the components of the instrument are experienced, despite the presence of sunshields. Every deviation of the temperature profile from the nominal configuration generates thermal stresses that cause deformations of the surfaces of the primary and secondary mirrors of the telescope. In turn, these deformations produce aberrations that may degrade the performance of the instrument. The effects of thermal stresses can be minimized with the employment of a suitable control strategy.

The objectives of the control strategy depend on the information available about the instrument. One objective, for example, is to maintain the initial temperature distribution. This method does not require wavefront sensing. Another possible objective is to achieve optimal performance of the instrument making use of the knowledge of the wavefront. Two different objective functions have been used in the present study. The first one is the norm of the temperature change. In other words, the matrix E of equation (11) is the identity matrix. This case is referred to as *temperature control.* The second performance index is the wavefront error (WFE) of the telescope. The wavefront error is a measure of the performance of the telescope and is defined below. This case is referred to as *WFE control*.

Under the assumption of the validity of linear theories, the deformations ξ induced by temperature changes on m thermal nodes can be written as

$$\xi = \bar{K} \cdot W \cdot (T_\alpha - T_0), \tag{34}$$

where W is the temperature-to-stress transformation matrix, and $\bar{K}$ is the pseudo-inverse of the stiffness matrix K. The nominal, zeros-stress temperatures of these nodes are the elements of T_0.

The Optical Path Difference vector of the telescope, (OPD), is defined as

$$OPD = \mathbf{O} \cdot \xi, \tag{35}$$

where $\mathbf{O}$ is the matrix of optical sensitivity to deformations for the system. Then, the wavefront error is defined as

$$w = \left((T_\alpha - T_0)^{\mathrm{T}} \cdot E \cdot (T_\alpha - T_0)\right)^{1/2} + w_0, \tag{36}$$

with E given by

$$E = (O \cdot \bar{K} \cdot W) \cdot (O \cdot \bar{K} \cdot W)^{\mathrm{T}}. \tag{37}$$

Since subtraction of heat requires expensive and complicated instrumentation, the telescope is assumed to operate on a nominal, 'hot' position, so that any rotation causes the temperatures to drop. Then, the desired temperature profile can be restored by adding heat to the system. Therefore, the constraints of the problem, equation (13), become

$$0 \leq Q_i, \quad i = 1, \ldots, m, \tag{38}$$

$$\sum_{i=1}^{m} Q_i \leq Q_{\mathrm{MAX}}, \tag{39}$$

where Q_{MAX} is the maximum available power from the heaters. In the thermal model of NGST there are $m = 798$ internal nodes that are used to model the primary mirror of the telescope. It is assumed that there are $q = 100$ available heaters.

Initially the instrument is at the 'hot' position. When it rotates, the temperature drops by a couple of degrees Kelvin. The induced thermal stresses generate a wavefront error equal to 107.58 nm. The initial and final (without control) profiles are plotted in Figure 2. The first step of the control strategy is to determine the location of the heaters. This is performed according to the procedure described in section 5.

Then, the optimal output of each heater is determined. As mentioned above, the goal of temperature control is to apply heat so that the final distribution is as close as possible to the initial (hot) distribution. Similarly, the goal of WFE control is to apply heat to maintain the error at the initial level. Application of temperature control produces a profile that is very close to the initial, 'hot', configuration, Figure 3. The required energy output from the heaters is 0.11 Watts. The final WFE after temperature control is reduced to 27.621 nm. On the other, hand WFE control results to a temperature profile that is very close to the 'cold' (without-control) profile, Figure 3. The required energy output is only 0.007 Watts, about 1/30 of the required energy for temperature control. The wavefront error after WFE control is 27.776 nm, just slightly higher than the error after temperature control.

The power output that is required from each heater is presented in Figure 4 for both control strategies. Finally, gray plots of the Optical Path Difference (OPD) with and without thermal control are shown in Figure 5. It can be observed that the OPD has been significantly reduced after employing the two proposed control strategies.

As regards the parameter updating problem, the proposed algorithm has been applied to SEAWINDS, a microwave radar that is used to measure near-surface wind speed and direction. The thermal model, shown in Figure 6, consists of $N = 150$ internal nodes, $n = 91$ boundary nodes, 66 linear conductors and 15392 radiators. The node vector of interest, T_α, consist of $m = 47$ nodes. The number of emissivities that have to be estimated is $M = 7$. These emissivities determine 85 radiators altogether. Two different values of these emissivities have been considered,

$$\Omega_{\mathrm{IN}} = [\,0.2 \quad 0.2 \quad 0.2 \quad 0.2 \quad 0.2 \quad 0.2 \quad 0.2\,]^{\mathrm{T}}, \tag{40}$$

and

$$\Omega_0 = [\,0.6 \ \ 0.05 \quad 0.35 \quad 0.45 \quad 0.5 \quad 0.35 \quad 0.4\,]^{\mathrm{T}}, \tag{41}$$

producing two different temperature profiles, T_{IN} and T_0. The difference of these two distributions across the nodes of interest is shown in Figure 7.

The test amounts to specifying T_0 as the target profile and trying to compute the emissivities that correspond to this profile, having Ω_{IN} and T_{IN} as starting point. In other words, it is assumed that Ω_{IN} is the initial estimate and that T_0 is the target profile, which the model must be able to calculate with updated emissivities.

The algorithm takes about 30 iterations to converge to the solution. The value of the cost function at the end of the computation is $2 \cdot 10^{-10}$. The maximum difference between T_0 and the temperature profile at the end of the computation is only $10^{-5}\ K$, Figure 8. The agreement between the calculated emissivities and Ω_0 is good up to the 5th significant digit. Similar tests were performed with different emissivities Ω_0. In all those tests, the algorithm recovered the desired parameters and temperature distributions with very good accuracy.

3. Concluding Remarks

Active thermal control and thermal-parameter updating are two common tasks that engineers are confronted with in aerospace applications. The present study was focused on developing techniques for the numerical treatment of these problems with network-based models. Temperature control and parameter updating are both formulated as nonlinear, constrained optimization problems. Numerical procedures for their treatment that are based on the Sequential Quadratic Programming (SQP) method offer important advantages such as flexibility, robustness and easy implementation.

In the present work, the SQP method has been employed in conjunction with analytic evaluation of the Jacobian of the governing set of equations, which provides significant savings on computing time. The proposed algorithms have been tested to large-scale thermal models of space-based science instruments, with quite promising results. The algorithms appear to be accurate and capable of achieving satisfactory convergence rate.

Acknowledgments This work was prepared by the Jet Propulsion Laboratory, California Institute of Technology, under a contract with the National Aeronautics and Space Administration.

References

1. DUSINBERRE, G.M., *Heat Transfer Calculations by Finite Differences*, International Textbook Company, Scranton PA, (1961).

2. BIRKHOFF, G., and KELLOGG, B. "Solution of equilibrium equations in thermal networks," *Proc. Sympos. on Generalized Networks*, pp. 443-452, Polytechnic Press, Brooklyn, New York, (1966).

3. RHEINBOLDT, W.C., *Methods for Solving Systems of Nonlinear Equations*, SIAM, Philadelphia, (1998).

4. MILMAN, M.H., and PETRICK, W., "A note on the solution to a common themral network problem encountered in heat transfer analysis of spacecraft," *Appl. Math. Model.*, Vol. **0**, pp. 00–00, (2000).

5. KRISHNAPRAKAS, C.K., "Efficient solution of spacecraft thermal models using preconditioned cojugate gradient methods," *J. Spacecraft Rockets*, Vol. **35**, pp. 760-764, (1998).

6. NARAYANA, N.B., BHANDARI, D.R., and MURTHY, H.N., "Thermal network correction by the optimization method," *J. Spacecraft Rockets*, Vol. **23**, pp. 542-544, (1986).

7. VARGA, R.S., *Matrix Iterative Analysis*, Prentice Hall, Englewood Cliffs, N.J., (1961).

8. MORÉ, J.J., " Nonlinear generalizations of matrix diagonal dominance with application to Gauss-Seidel iterations," *SIAM J. Num. Anal.*, Vol. **9**, pp. 357–378, (1972).

9. KELLER, H.B., *Lectures on Numerical Methods in Bifurcation Problems*, Springer Verlag, Berlin, (1987).

10. BRYSON, A.E., and HO, Y.C., *Applied Optimal Control*, Taylor and Francis, Bristol PA, (1975).

11. GILL, P.E., MURRAY, W., and WRIGHT, M.H., *Practical Optimization*, Academic Press, London, (1981).

12. HAN, S.P., "A Globally Convergent Method for Nonlinear Programming," *J. Opt. Th. Appl.*, Vol. **22**, p. 297, (1977).

13. POWELL, M.J.D., "Algorithm for NonLinearly Constrained Optimization Calculations," *Numerical Analysis*, Springer Verlag, Vol. **630**, (1978).

14. MATLAB, *Optimization Toolbox Manual*, Mathworks Inc., (1998).

15. NEEDELS, L. (editor), *IMOS: Integrated Modeling of Optical Systems, User's Manual*, Jet Propulsion Laboratory, (2000).

16. FLETCHER, R., *Practical Methods for Optimization*, J. Wiley and Sons, New York, (1987).

Figure Captions

Figure 1: Schematic of the NGST thermal model and initial temperature distribution.

Figure 2: Initial and final (without control) temperature distributions.

Figure 3: Difference between initial and final temperature distributions with and without control.

Figure 4: Heat output from each heater after temperature and wavefront error control.

Figure 5: Optical Path Difference (OPD) without control and after control.

Figure 6: Schematic of the SEAWINDS instrument.

Figure 7: Actual and optimal temperature distribution on the SEAWINDS instrument.

Figure 8: Difference between optimal and calculated distributions after application of the parameter-updating algorithm on the SEAWINDS instrument.

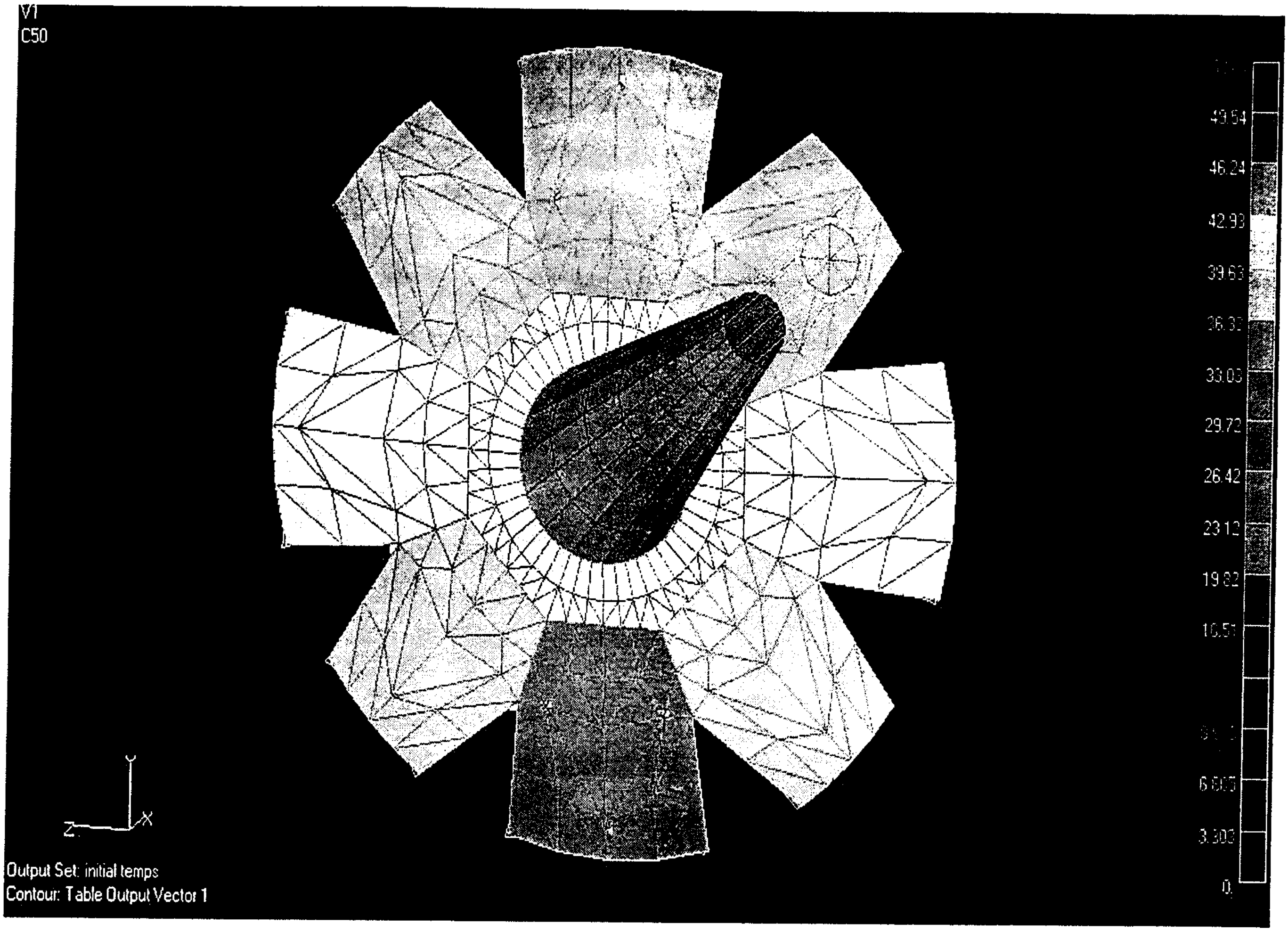
V1
C50
49.54
46.24
42.93
39.63
36.33
33.03
29.72
26.42
23.12
19.82
16.51
6.605
3.303
0.
Y
Z
X
Output Set: initial temps
Contour: Table Output Vector 1

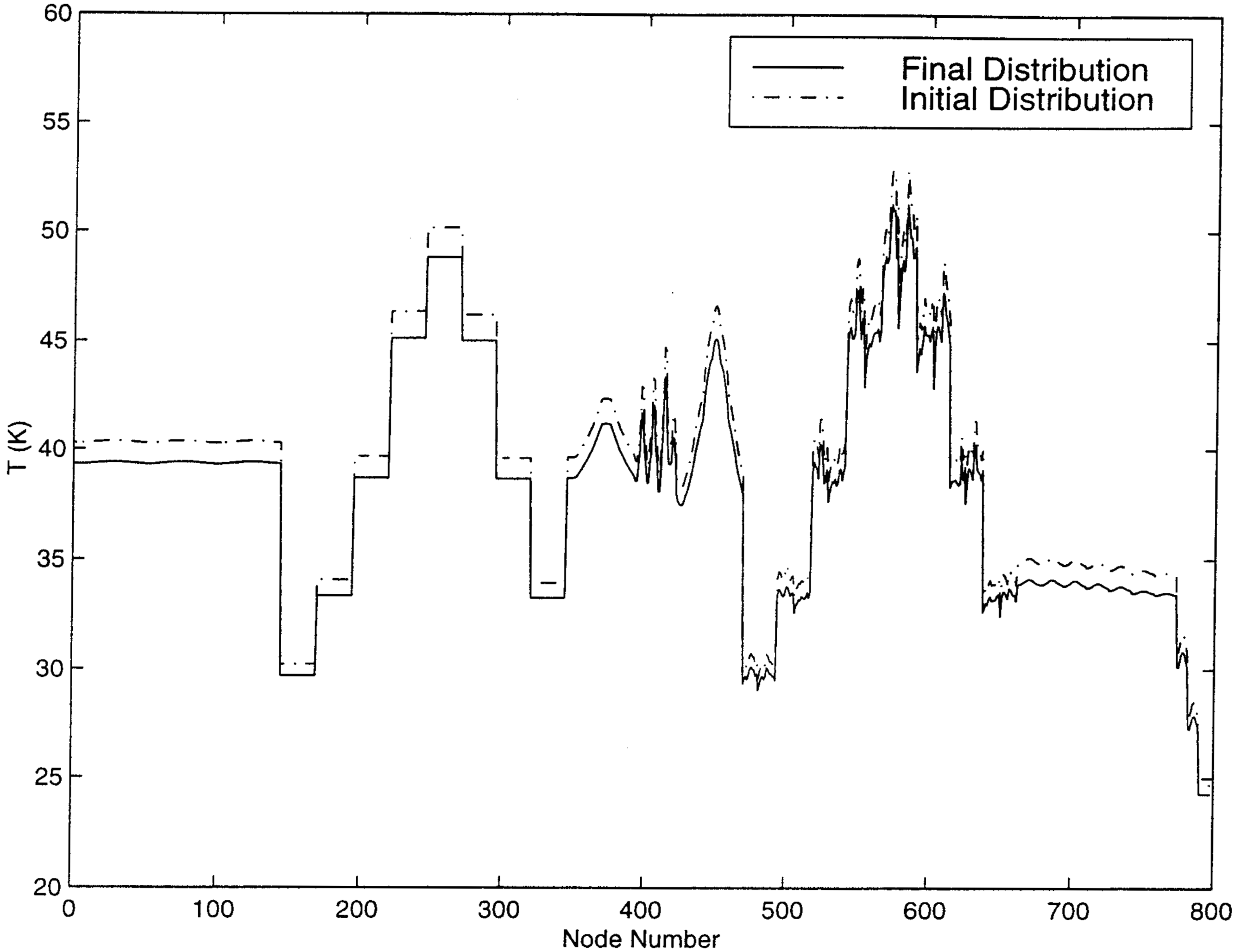

Final Distribution
Initial Distribution
60
55
50
45
40
35
30
25
20
T (K)
0
100
200
300
400
500
600
700
800
Node Number

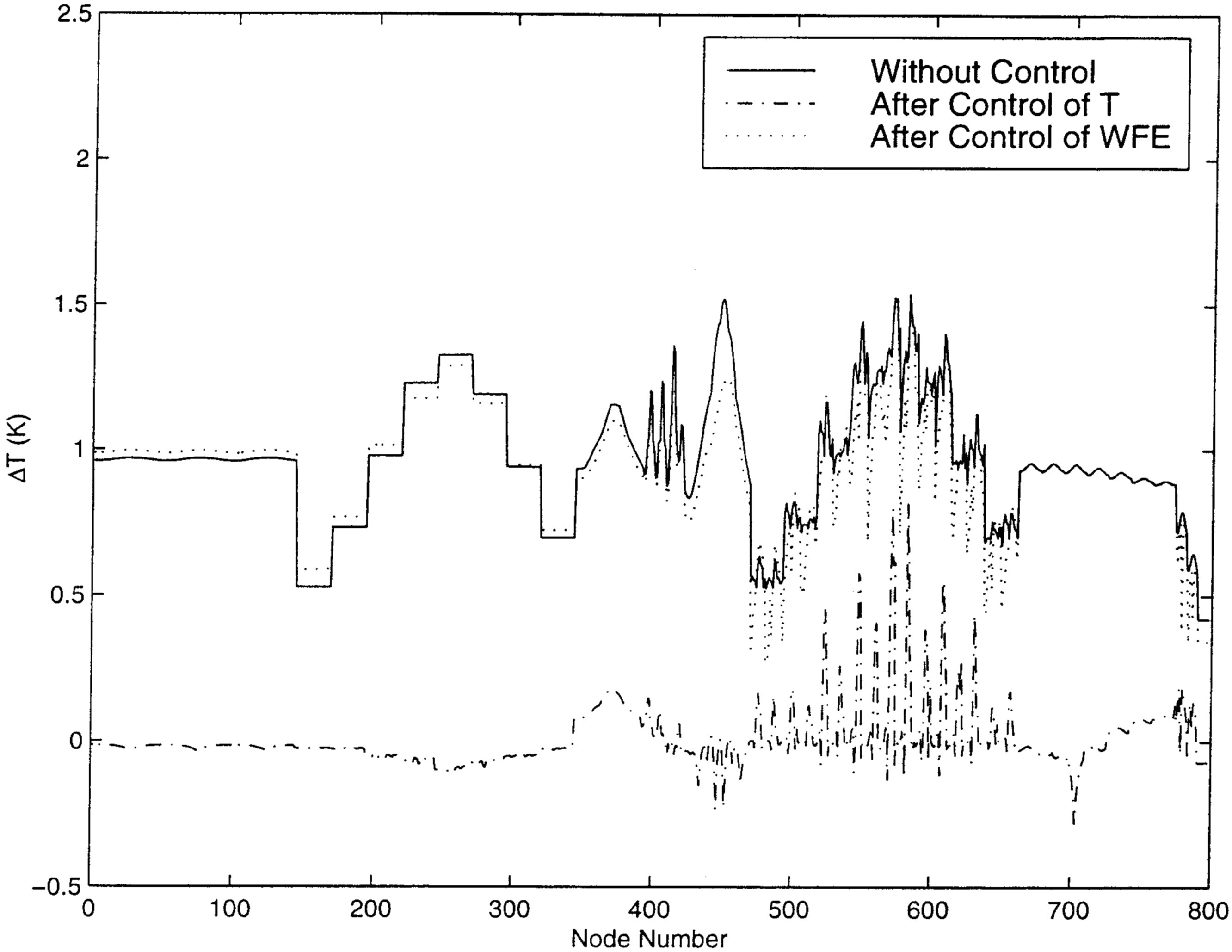

Without Control
After Control of T
After Control of WFE
ΔT (K)
Node Number
2.5
2
1.5
1
0.5
0
−0.5
0
100
200
300
400
500
600
700
800

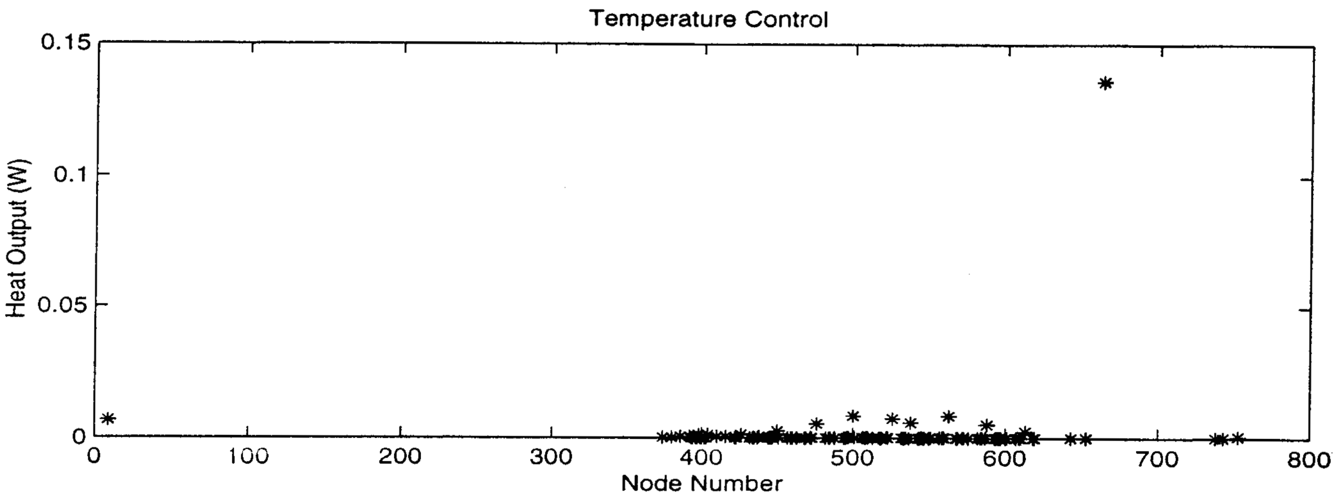
Temperature Control
0.15
0.1
0.05
0
Heat Output (W)
0
100
200
300
400
500
600
700
800
Node Number

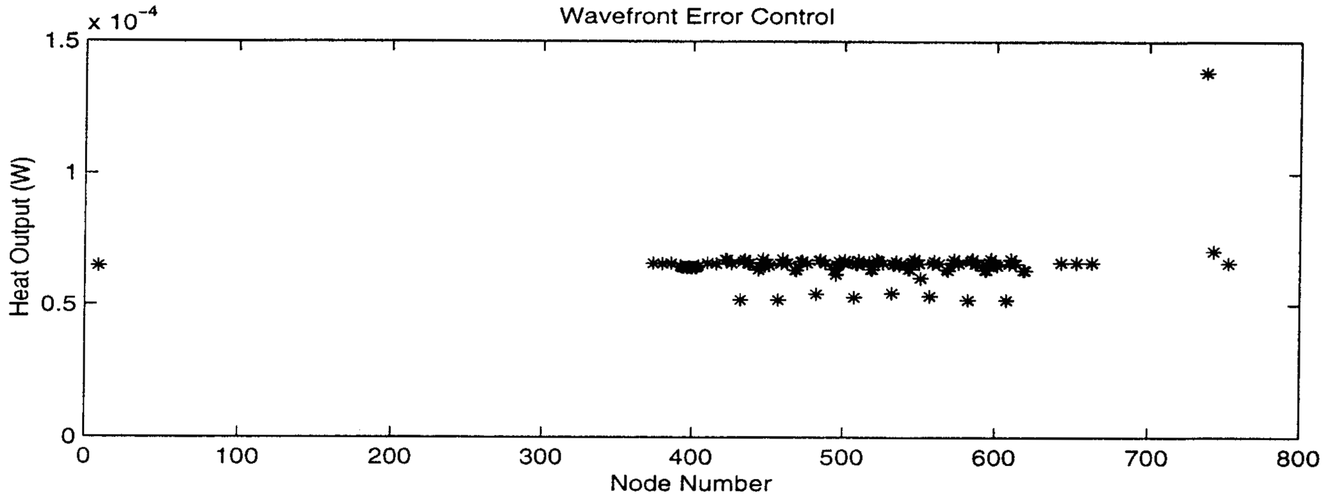
Wavefront Error Control
x 10^-4
1.5
1
0.5
0
Heat Output (W)
0
100
200
300
400
500
600
700
800
Node Number

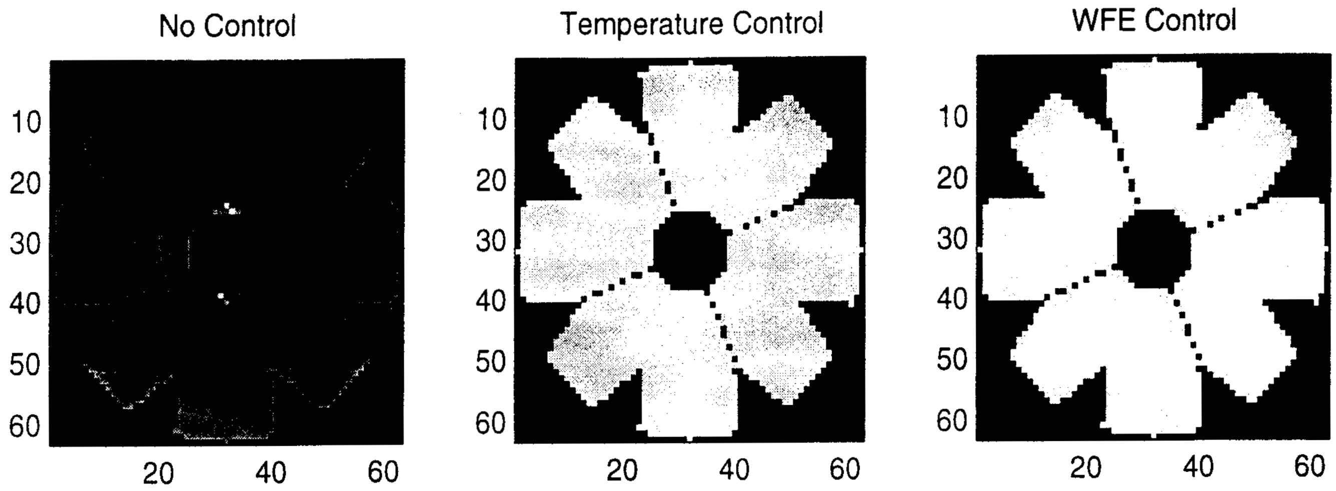
No Control
Temperature Control
WFE Control
10
20
30
40
50
60
20
40
60

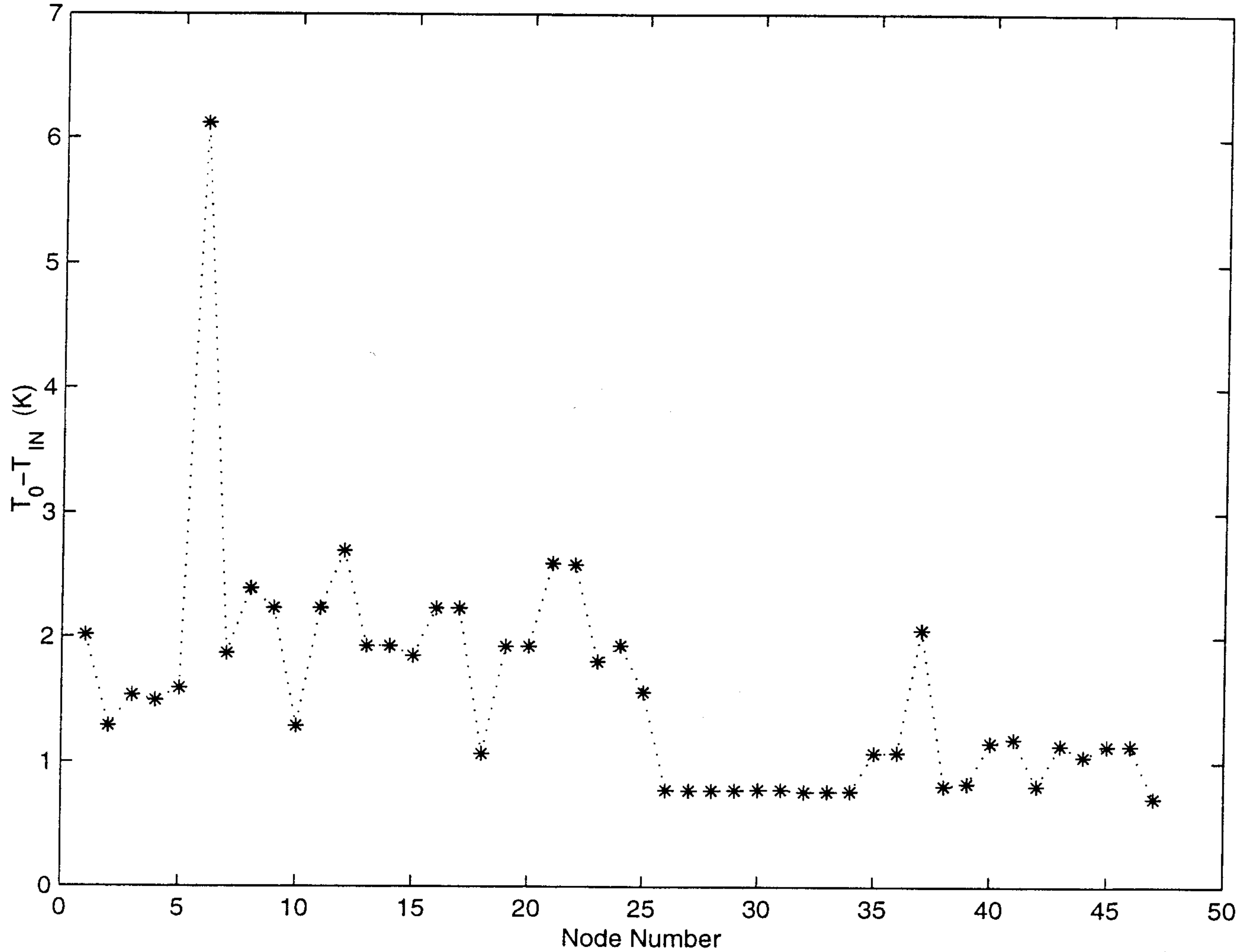

7
6
5
4
3
2
1
0
T_0-T_{IN} (K)
0
5
10
15
20
25
30
35
40
45
50
Node Number

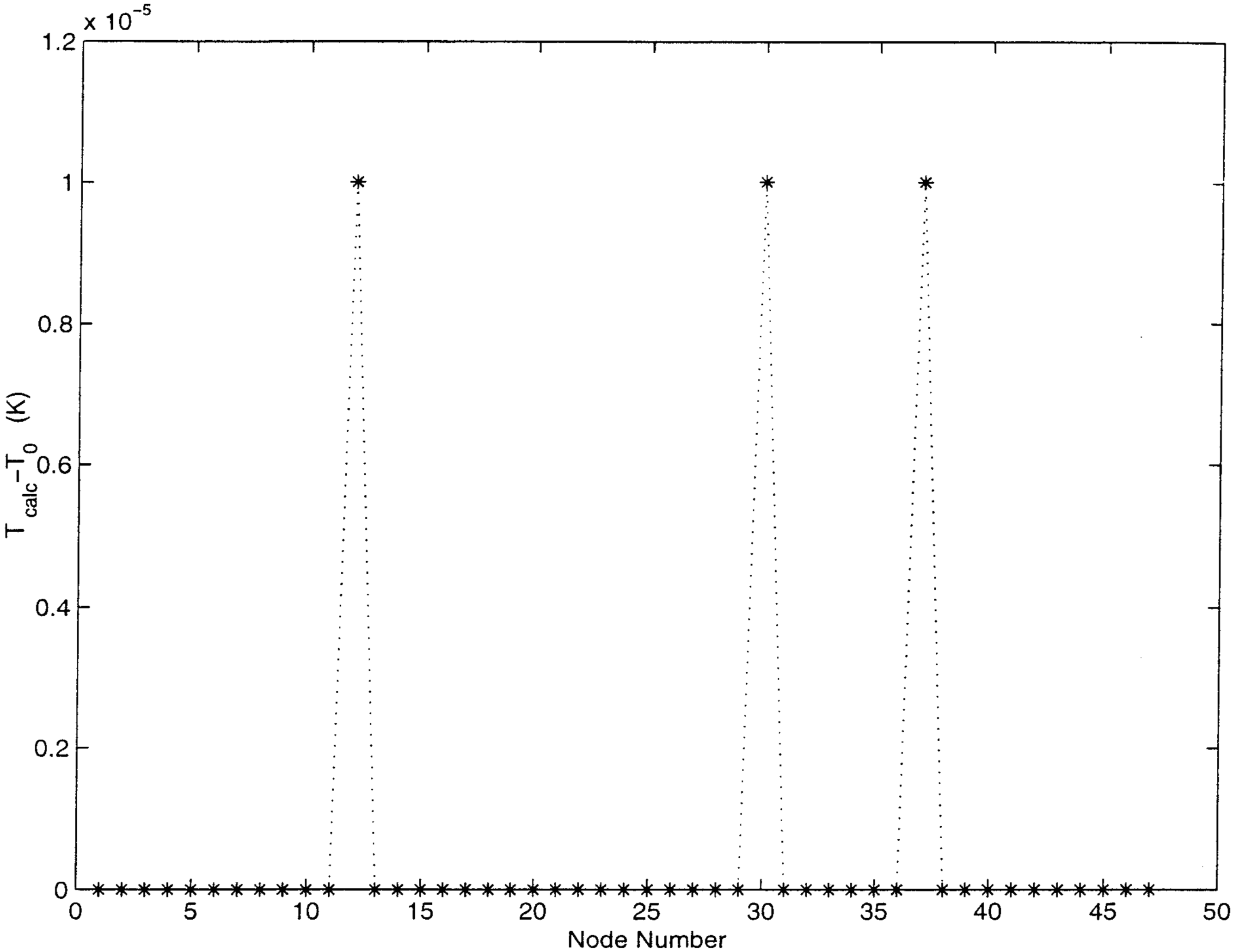
x 10^-5
1.2
1
0.8
0.6
0.4
0.2
0
T_calc−T_0 (K)
0
5
10
15
20
25
30
35
40
45
50
Node Number